analytical chemistry

Article

pubs.acs.org/ac

Noninvasive Body Fat Burn Monitoring from Exhaled Acetone with Si-doped WO_3-sensing Nanoparticles

A. T. Güntner,[†] N. A. Sievi,[‡] S. J. Theodore,[†] T. Gulich,[†] M. Kohler,[‡] and S. E. Pratsinis*[,†]

[†]Particle Technology Laboratory, Department of Mechanical and Process Engineering, Eidgenössische Technische Hochschule Zürich, CH-8092 Zürich, Switzerland

[‡]Department of Pulmonology, University Hospital Zürich, CH-8091 Zürich, Switzerland

Supporting Information

ABSTRACT: Obesity is a global health threat on the rise, and its prevalence continues to grow. Yet suitable biomedical sensors to monitor body fat burn rates in situ, to guide physical activity or dietary interventions toward efficient weight loss, are missing. Here, we introduce a compact and inexpensive breath acetone sensor based on Si-doped WO_3 nanoparticles that can accurately follow body fat burn rates in real time. We tested this sensor on 20 volunteers during exercise and rest and measured their individual breath acetone concentrations in good agreement with benchtop proton transfer reaction time-of-flight mass spectrometry (PTR-TOF-MS). During exercise, this sensor reveals clearly the onset and progression of increasing breath acetone levels that indicate intensified body fat metabolism, as validated by parallel venous blood β-hydroxybutyrate (BOHB) measurements. Most importantly, we found that the body fat metabolism was especially pronounced for most volunteers during fasting for 3 h after exercise, with strong variation between subjects, and this was displayed correctly by the sensor in real-time. As a result, this simple breath acetone sensor enables easily applicable and hand-held body fat burn monitoring for personalized and immediate feedback on workout effectiveness that can guide dieting as well.

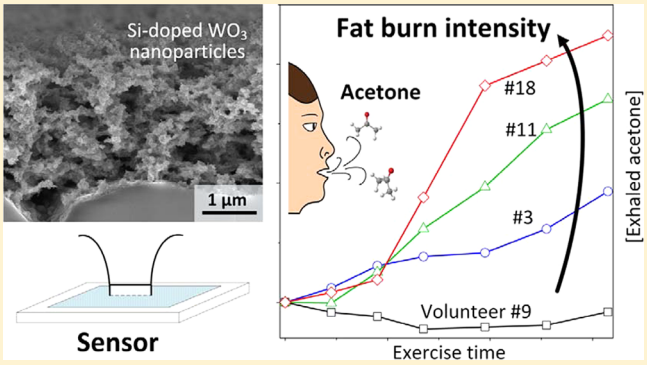

Worldwide, 15% of women and 11% of men were obese [body mass index (BMI) $\geq$ 30 kg·m^{-2}] in 2014,[1] with increasing numbers in most countries.[2] Unfortunately, conventional technologies either fail to indicate body fat burn rates in situ, to guide physical activity and dietary interventions, or are too costly for widespread application (e.g., indirect calorimetry). Analyzing volatile organics in human breath opens exciting new avenues for the next generation of health monitoring devices.[3] In particular, measuring exhaled acetone, a volatile byproduct of lipolysis,[4] with a portable device could enable such personal body fat burn monitors.[5] With breath analysis being noninvasive, user-friendly (similar to sweat analysis),[6] and always accessible,[7] it might be ideal for easy and routine application in gyms or at home.

Breath acetone had been measured already with gas chromatographic[8] and mass spectrometric techniques,[9−12] chemical adsorption columns,[13] and electronic noses.[14] However, these are expensive with limited portability,[8−12] for single use only with long response time (>5 min),[13] or just inaccurate,[14] and thus are hardly suitable for routine measurements with personal monitors. Modern chemoresistive gas sensors are promising candidates for personal breath analyzers due to their extremely compact design,[15] high gas sensitivity when nanostructured,[16,17] and current use in breath analysis (e.g., hemodialysis monitoring).[18] However, the challenge remains to design a sensing material selective for acetone for reliable detection in the complex matrix of human breath (872 compounds identified previously).[19]

Here, we report a portable breath acetone sensor based on Si-doped ε-WO_3 nanoparticles to monitor body fat burn rates in real time during exercise and rest. This material was selected for its high thermal stability,[20] superior sensitivity,[21] and selectivity[22] to acetone at high relative humidity (e.g., 90%). We evaluated this sensor in combination with a tailor-made sampler for reproducible breath extraction on 20 volunteers and measured their individual breath acetone profiles. These results were closely compared to simultaneously measured breath analysis by state-of-the-art proton transfer reaction time-of-flight mass spectrometry (PTR-TOF-MS) to assess the sensor's accuracy and parallel venous blood β-hydroxybutyrate (BOHB) to confirm the relationship to fat metabolism activity.

EXPERIMENTAL SECTION

Acetone Sensor Fabrication and Film Characterization. The Si-doped (10 mol %) ε-WO_3 nanoparticles were prepared by flame spray pyrolysis (FSP) and directly

Received: July 20, 2017
Accepted: September 11, 2017
Published: September 11, 2017

DOI: 10.1021/acs.analchem.7b02843
Anal. Chem. 2017, 89, 10578−10584

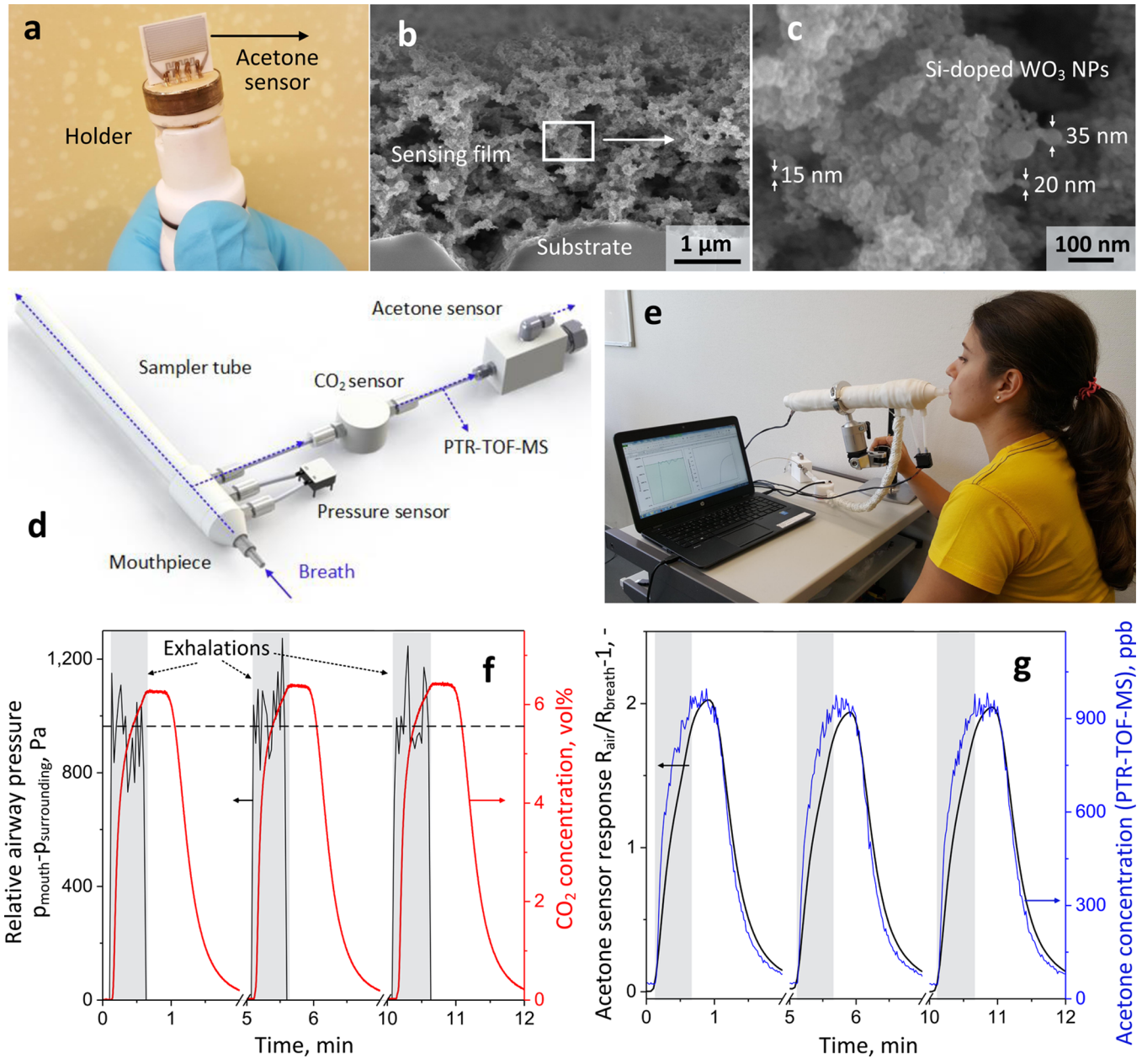

Figure 1. Breath analyzer for noninvasive body fat burn monitoring. (a) Compact acetone sensor mounted on a Macor holder. (b) Scanning electron microscopy exhibits the highly porous morphology of the sensing film (cross-section) (enlarged in panel c) formed by aggregated, acetone-selective Si-doped WO_3 nanoparticles (NPs). (d) Breath analyzer combining the acetone sensor with a sampler to extract breath in a standardized fashion. The sampler comprises a tube to capture and buffer end-tidal breath, a pressure sensor to monitor the relative airway pressure, and a CO_2 sensor. Parallel PTR-TOF-MS analysis just before the acetone sensor is performed for cross-validation. (e) Breath analyzer in operation: the subject exhales into the sampler tube and receives prompt visual feedback on airway pressure, duration, and acetone sensor analysis. (f) Sensor signals for relative airway pressure (black line) and CO_2 (red line) for three 30 s exhalations (gray-shaded) of a subject. The target airway pressure of 980 Pa (dashed line) is maintained well, corresponding to a flow of 50 mL·s^{-1}. (g) Acetone sensor responses (black line) and concentrations from PTR-TOF-MS (blue line). Both provide comparable acetone measurement in real time. Note that sensor response is defined as $R_{air}/R_{breath} - 1$, where R_{air} is sensor film resistance in surrounding air and R_{breath} is sensor film resistance when exposed to the breath sample.

deposited[23] onto Al_2O_3 substrates with interdigitated electrodes.[20] The FSP precursor solution consisted of ammonium metatungstate hydrate (Sigma–Aldrich, purity ≥97%) and hexamethyldisiloxane (Sigma–Aldrich, purity ≥98%) to obtain the nominal Si content. This was diluted by a 1:1 mixture of ethanol (Sigma–Aldrich, purity ≥99.8%) and diethylene glycol monobutyl ether (Sigma–Aldrich, purity ≥98%) to achieve a final metal (W and Si) concentration of 0.2 M. This precursor is fed at 5 mL·min^{-1} through a FSP nozzle and dispersed (1.5 bar pressure drop) by 5 L·min^{-1} oxygen to a fine spray ignited by a ring-shaped flame of premixed methane/oxygen (1.25/3.2 L·min^{-1}) while additional sheath oxygen was supplied at 5 L·min^{-1}. The Al_2O_3 substrates featured dimensions of 15 × 13 × 0.8 mm and had a set of interdigitated electrodes (spacing 350 µm) and a Pt resistance temperature detector (RTD) on the front side. A Pt heater to control the temperature was placed on the back. The morphology of the sensing films was characterized by scanning electron microscopy (SEM) with a

DOI: 10.1021/acs.analchem.7b02843
Anal. Chem. 2017, 89, 10578–10584

Hitachi FE-SEM 4000 operated at 5 kV. To investigate the film's cross-section, the sensors were split prior to the measurement.

Breath Sampler Design. The sampler is illustrated in Figure 1d. It comprised a disposable and sterile mouthpiece (EnviTeC-Wismar) connected to an open-ended sampler tube, with inner diameter 25 mm and length 375 mm, to sample and buffer[24] end-tidal breath. A flow restrictor (1.4 mm orifice) was installed inside the sampler tube just behind the mouthpiece, and the relative airway pressure ($p_{mouth} - p_{surrounding}$) was measured with a differential pressure sensor (SDP series, Sensirion) at the orifice. A transfer line (d_i = 6 mm) was connected to the sampler tube to extract breath sample for the acetone sensor and PTR-TOF-MS. A CO_2 sensor (Capnostat 5, Respironics) was placed in the transfer line to monitor the breath portions. All surfaces in contact with the breath were either disposable (mouthpiece) or made of inert Teflon and heated to 60 °C to avoid analyte adsorption and water condensation to minimize cross-contamination.

Breath and Blood Analysis. Sampled breath was analyzed in real time with the acetone sensor and PTR-TOF-MS simultaneously. Therefore, the acetone sensor was mounted on a Macor holder and installed in a Teflon chamber, both tailor-made with a design described in detail elsewhere.[21] The chamber was connected to the breath sampler via the transfer line, as shown in Figure 1d. The sensor was fed with a constant flow of 130 mL·min^{-1} by a vane pump (SP 135 FZ, Schwarzer Precision) connected to the sensor chamber's exhaust. A direct current (dc) source (R&S HMC8043) was applied to heat the acetone sensor to its optimal temperature of 350 °C[21] while that was monitored continuously by the substrate's RTD. Sensing film (ohmic) resistances were measured and recorded with a multimeter (Keithley 2700). The PTR-TOF-MS 1000 (Ionicon Analytik, Austria) was fed from the sensor transfer line with sample extraction just before the acetone sensor (Figure 1d). The ionization conditions were 600 V drift voltage, 60 °C drift temperature, and 2.3 mbar drift pressure. Acetone (CAS 67-64-1) concentrations were determined in the H_3O^+ mode by measuring the counts per second at a mass-to-charge ratio of 59.049[25] and comparing them to calibration curves determined routinely before the breath tests with a calibrated acetone gas standard (10 ppm in synthetic air, Pan Gas 5.0). Venous blood samples were analyzed for BOHB (CAS 300-85-6) concentration by the Institute of Clinical Chemistry, University Hospital Zurich.

Study Design. A cohort of 20 volunteers (13 male and 7 female), age 20−33 years, participated in this study. All were healthy and had a body mass index between 18.3 and 27.7 kg·m^{-2} (for detailed information see Table S1). None of the participants had any respiratory symptoms; however, one was a smoker (subject 9) and another was asthmatic (subject 7). Earlier results suggested no influence of smoking on breath acetone concentrations,[26] while there is no evidence that asthma affects it either. Note that pulmonary function tests may provide quantitative information about respiratory health status,[27] but this was not performed here. Diabetics were excluded due to their disordered metabolism and known altered breath acetone levels.[28] Each subject had been informed about the proceeding and signed a consent form prior to the tests. This study had been approved by the Kantonale Ethikkommission Zürich. The volunteers were asked in advance to fast for 12 h, not to brush their teeth nor use mouthwash for 2 h, and stay abstinent from alcoholic beverages for 24 h before and during the experiment to avoid exogenous interference. Each volunteer was tested twice on different days. The first test (denoted as exercise) consisted of 3 × 30 min initial moderate physical activity, with 15 min breaks in between for breath and venous blood sampling, followed by 3 h of rest. The second test (denoted as control) followed the same protocol, however, this time without initial exercise but staying at rest throughout the entire testing course. Physical activity was performed on a bicycle ergometer (E5, Kettler) with power-independent pedal speed and heart rate control with a pulse belt (T34, Polar). The workload was adapted automatically by the ergometer to maintain a heart rate at 63%[29] of maximum heart rate (HR_{max}) at 60−80 rpm. HR_{max} (in beats per minute, bpm) was approximated for men by $HR_{max} = 223 - 0.9x$ and for women by $HR_{max} = 226 - x$, with x representing the subject's age (in years). Breath was sampled in total seven times: just before physical activity, after each 30 min of physical activity, and thereafter every 60 min during rest. Experiments were performed in a ventilated room to avoid accumulation of exogenous compounds (e.g., acetone) in the room air. Background acetone concentrations did not exceed 100 parts per billion (ppb). Venous blood samples were taken three times: before and after physical activity and at the end of the test.

RESULTS AND DISCUSSION

Breath Acetone Sensor Design. The employed compact and inexpensive sensor features a thin Si-doped WO_3 sensing film on top of interdigitated electrodes (Figure 1a). Such films are highly porous (Figure 1b), consisting of a fine structure of Si-doped WO_3 nanoparticles (Figure 1c), typical for such flame-made layers.[30,31] The open structure of the sensing film allows gas molecules to diffuse rapidly through the film for fast response and recovery times, suitable for breath analysis in real time.[21] Also, it provides a large surface area to sense acetone even at low concentrations (e.g., 20 ppb),[21] sufficient for breath acetone detection, with levels typically above 150 ppb.[11] In principle, such semiconductive metal oxide nanoparticles are chemoresistive-type gas sensors. In other words, analytes (e.g., acetone) interact with surface species of the metal oxide, modulating the film resistance and resulting in a detectable sensor response.[32] Specifically for WO_3, analyte interaction with lattice oxygen at the surface may dominate.[33] Most remarkably, since these surface interactions are reversible, such sensors are suitable for multiple[21] and even continuous breath analyses.

Given the complexity of breath, a key challenge in sensor development is sufficient selectivity to acetone to ensure an accurate measurement. Here, we address this by applying ferroelectric ε-WO_3 exhibiting high acetone selectivity.[34] This is probably due to strong interaction between the spontaneous electric dipole moment of ε-WO_3 with the high dipole moment of acetone.[34] The metastable ε-WO_3 is stabilized by Si doping (10 mol %)[20] without using potentially toxic elements (e.g., Cr).[34] Such sensors had been evaluated already in simulated breath mixtures to detect various acetone concentrations[21] and showed promising results in offline[35] and online[21] breath tests with a portable analyzer.[36]

Breath Sampling and Analysis Strategy. Reliable acetone analysis requires standardized breath sampling, since different breathing maneuvers and sample volume affect acetone concentration.[5] Therefore, a novel sampler was designed (Figure 1d,e; see Experimental Section) to extract

DOI: 10.1021/acs.analchem.7b02843
Anal. Chem. 2017, 89, 10578−10584

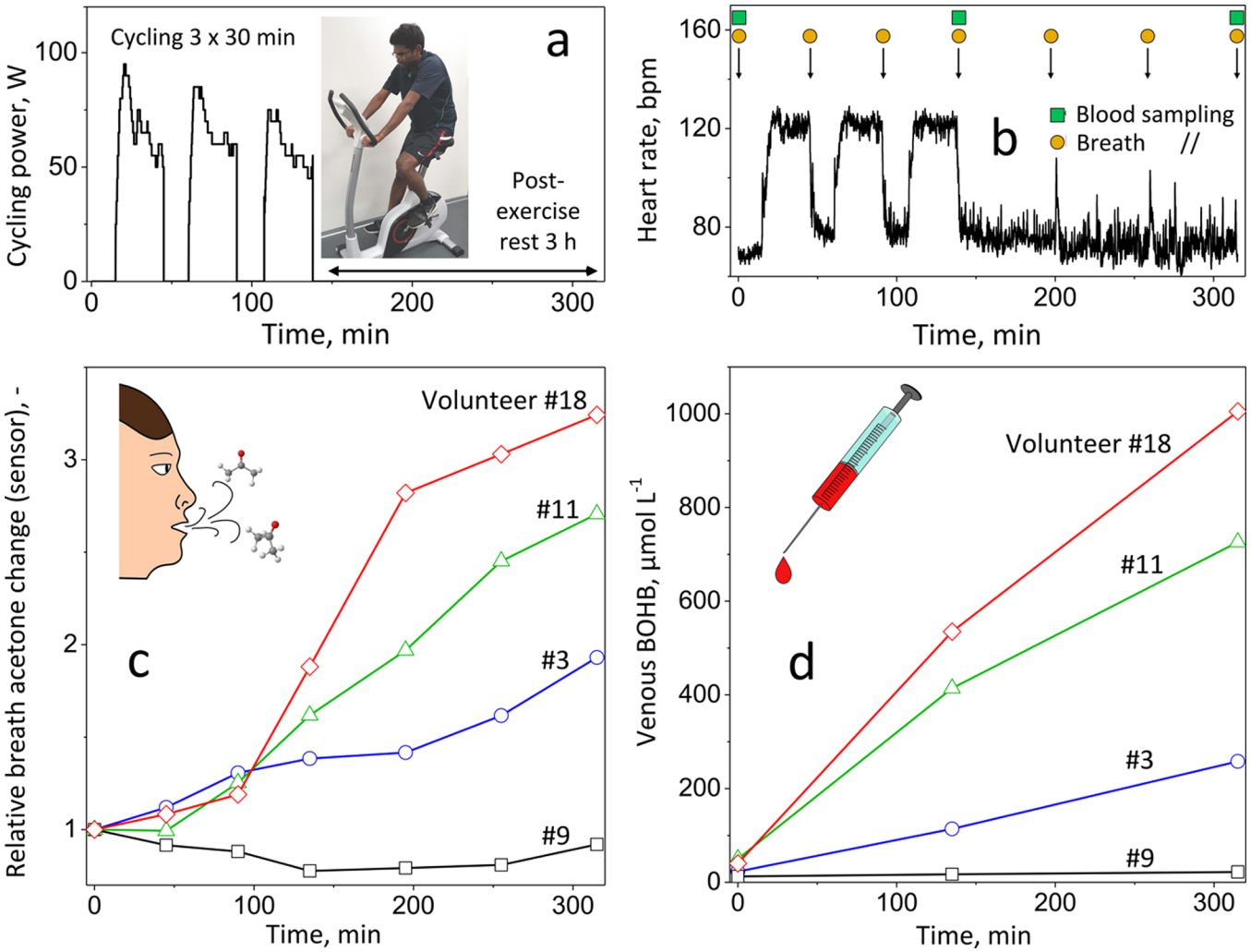

Figure 2. Body fat burn monitoring during exercise and rest. Typical cycling power profiles (a) and heart frequency (b) of a subject when undergoing the testing course, with 3 × 30 min cycling on an ergometer to stimulate body fat metabolism and 3 h postexercise rest, are shown. Note that the load is adjusted automatically during cycling to keep the subject always at approximately 63% of the maximum heart rate. Symbols in panel b indicate breath (orange circles) and venous blood (green squares) sampling. (c) Individual breath acetone changes (relative to initial value) measured by the sensor of representative subjects during the testing course. (d) Corresponding venous blood β-hydroxybutyrate (BOHB) concentrations that were sampled only three times instead of seven as with breath (in panel b) to minimize the discomfort for the volunteers.

reproducible end-tidal breath in a monitored fashion (by relative airway pressure and CO_2 concentration) with minimal effort for the subject. While early breath involves air from the mouth and upper airways (anatomic dead space), most relevant and highest acetone levels occur in the later portions from the bronchi and pulmonary alveoli (end-tidal breath) containing chemical information about blood composition (including metabolic products) due to gas exchange in the lung.[37] In principle, complete breath is exhaled through an open-ended sampler tube. After exhalation, only the end-tidal portion remains inside the tube and is fed to the sensor for prolonged exposure, as can be evaluated from the CO_2 profiles (Figure 1f, red line) of three consecutive exhalations (each 30 s) of a subject. During exhalation, the CO_2 concentration increases rapidly until it reaches a maximum at 6.2−6.4%, indicative of end-tidal breath (CO_2 > 3%).[38] Most importantly, this portion is buffered for an additional 20 s after exhalation before the CO_2 level declines rapidly and stabilizes again at the initial baseline indicating fast and complete refreshment or regeneration of the sampler tube.

Figure 1g shows the corresponding acetone sensor responses (black line) and concentrations measured by PTR-TOF-MS (blue line). Both instruments respond immediately with reproducible results for the three breath samples. Specifically, the acetone sensor response increases rapidly and reaches each time a maximum at a response of ∼2 during the prolonged exposure to end-tidal breath. This corresponds to an acetone level of ∼960 ppb, as measured by PTR-TOF-MS, and it is within typical daily variation.[11] While the sensor features slower response times than the PTR-TOF-MS, it is still sufficiently fast to detect the acetone reliably with the present sampler. The sensor shows also higher (>5 times) signal-to-noise ratio than PTR-TOF-MS, a favorable feature for signal analysis. After exposure, the sensor and PTR-TOF-MS always recover the initial baseline, similar to CO_2 (Figure 1f, red line), and are ready for reuse.

Individual Body Fat Burn Monitoring during Exercise and Rest. The sampler-sensor system was applied to monitor the breath acetone dynamics of 20 volunteers during exercise and postexercise rest. Therefore, all subjects underwent exercise with initial three times 30 min cycling on an ergometer at

DOI: 10.1021/acs.analchem.7b02843
Anal. Chem. 2017, 89, 10578−10584

moderate intensity (Figure 2a,b, please see Experimental) to stimulate their body fat metabolism followed by a 3 h rest. Prior to and throughout the testing course, the volunteers have been fasting to minimize the influence of food intake. The corresponding breath acetone profiles of four representative volunteers (for physiological data of all subjects, please see Table S1) are shown in Figure 2c. Note that breath acetone is indicated as relative change from the initial value (at $t = 0$) to evaluate only the effect of the exercise. That way, also a comparison between subjects is easier, as their initial acetone concentrations may vary significantly due to biological variability.[11]

In a typical case (e.g., subject 18, red diamonds), breath acetone increases only little during exercise but triples during the postexercise rest. Increasing breath acetone concentrations during and after exercise have been observed also in other studies (e.g., during cycling[8] and walking[10]) and should reflect enhanced body fat metabolism, with acetone being a byproduct of lipolysis.[4] Thus, for subject 18, it seems that the initial exercise stimulated body fat metabolism that becomes most pronounced after exercise. To confirm this, venous blood β-hydroxybutyrate (BOHB) is analyzed simultaneously, as a marker for body fat metabolism[5] (Figure 2d). Remarkably, it shows the same dynamic response, supporting that the present breath acetone sensor indeed follows body fat metabolism but, most importantly, in a noninvasive manner.

Individual body fat burn rates may differ between humans due to the usual biological variability (including different fitness levels). Nevertheless, the sensor should recognize this correctly for customized feedback. In fact, when comparing the individual exercise profiles of selected volunteers (Figure 2c), distinctly different breath acetone profiles are detected, again all in good agreement to BOHB dynamics (Figure 2d). For instance, subject 3 (blue circles) shows a steady breath acetone increase already during exercise with higher concentrations during the postexercise rest, similar to subject 18 though at a lower level. On the other hand, the breath acetone of subject 9 (black squares) is hardly affected by exercise. In fact, it even decreases slightly during exercise. Note that this may be affected by the smoking habit of subject 9 (see Table S1); however, the breath acetone dynamic is rather similar to that of nonsmoking subject 4 (see Figure S1a), and previous studies have suggested no influence of smoking on breath acetone concentrations.[26] From these results, already some feedback can be provided to the subjects: while the workout stimulated the body fat metabolism of subjects 3, 11, and 18 with highest rates during the postexercise rest, it was not effective for subject 9. In a next step, this device could be used to guide the optimization of their training conditions (e.g., higher cycling intensity, type of exercise, etc.) to maximize the individual body fat metabolism.

For comparison, each volunteer was tested also another time following the same protocol but without cycling (denoted as control). Figure 3a shows the average breath acetone change and variability of the 20 subjects when tested with exercise (red triangles) and as control (blue squares). While the volunteers responded on average with a breath acetone increase, especially after exercise, the sensor detects only a small breath acetone change toward the end of the measurement for control, probably due to the prolonged fasting of the volunteers[12,39] (see Figure S1 for individual breath acetone data). Both trends are again in agreement with the measured venous blood BOHB (Figure 3b), including for the controls with the small increase

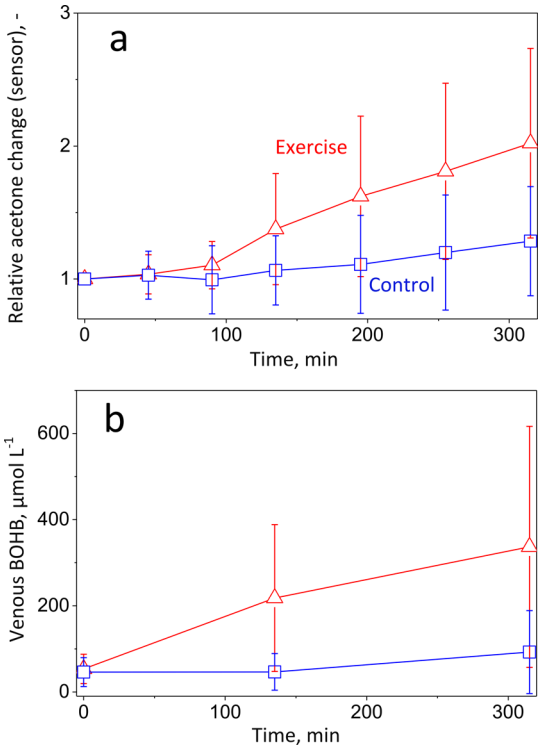

Figure 3. Breath and venous blood data of 20 subjects: average acetone change measured by (a) sensor and (b) venous blood β-hydroxybutyrate (BOHB) concentrations during testing with 3 × 30 min initial exercise and 3 h rest (red triangles). For comparison, each subject is tested a second time as control (blue squares) following the same protocol without exercise. Error bars indicate the standard deviations of 20 volunteers.

toward the end of the measurement, indicating enhanced fat metabolism.[4] Note that error bars in Figure 3a,b partially overlap, resulting from the different individual body fat burn rates (and thus breath acetone and venous blood BOHB profiles) in response to the exercise and control conditions due to the volunteers' biological variability.

To evaluate the correlation between the sensor-measured breath acetone and venous blood BOHB in more detail, Figure 4a shows the corresponding scatter plot of all data points. Breath acetone and BOHB correlate well with correlation coefficients of 0.82 ($p < 0.05$). This is quite comparable to other studies that found an average of 0.88 (there, however, for absolute concentrations).[5] This provides further evidence that breath acetone is a suitable surrogate for body fat burn and the presented sensor monitors it noninvasively.

Finally, to cross-validate the sensor's accuracy for breath acetone detection, all breath samples were analyzed simultaneously by PTR-TOF-MS. Figure 4b shows the scatter plot for relative acetone change as measured by the sensor and PTR-TOF-MS for all 280 breath samples (for PTR-TOF-MS-measured acetone concentrations over time, see Figure S2). Both instruments correlate strongly (correlation coefficient 0.97, $p < 0.05$) and agree well without systematic bias and sufficiently small limits of agreement, as indicated by additional Bland–Altman analysis[40] (see Figure S3). Small sensor underprediction occurs only at higher acetone changes [compare fitted (dashed) and ideal (solid) lines in Figure 4b]. As a result, our sensor reliably detects and monitors breath acetone. This is remarkable considering the sensor's compact-

DOI: 10.1021/acs.analchem.7b02843
Anal. Chem. 2017, 89, 10578–10584

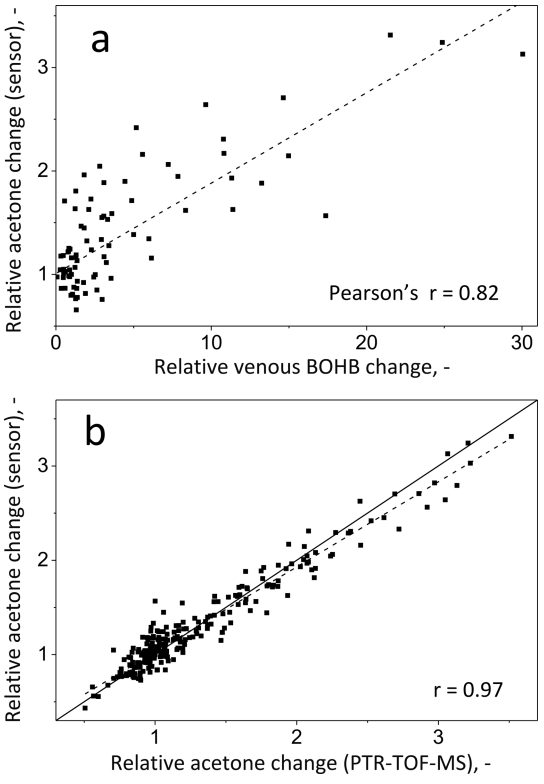

Figure 4. Scatter plots indicating correlations of relative acetone change measured by the sensor and (a) venous blood BOHB or (b) relative acetone change measured by PTR-TOF-MS. Corresponding Pearson's (r) correlation coefficients along with fitted trend lines (dashed) and ideal line (solid line in panel b) are indicated as well.

ness and low cost compared to PTR-TOF-MS. At the same time, it is more accurate than chemical adsorption columns, which are hand-held breath acetone detectors but for single use.[13]

CONCLUSIONS

A portable, easy-to-use, and inexpensive breath acetone sensor is presented that can monitor in situ body fat burn dynamics during exercise and rest. It consists of an extremely porous film of flame-made Si-doped WO_3 nanoparticles for highly sensitive, selective, and rapid breath acetone detection. To facilitate reproducible and reliable breath acetone analysis, a sampler that extracts and buffers the end-tidal fraction of breath for prolonged sensor exposure was crucial. When applied to 20 volunteers during exercise and rest, this sensor recognized and closely followed individual breath acetone concentrations, in good agreement with benchtop PTR-TOF-MS. Increasing breath acetone reflected intensified body fat metabolism, as confirmed by measured venous blood BOHB. Most remarkably, the strongest body fat burn with significant intraindividual variation was detected typically during a 3 h postexercise rest. As a result, this compact breath analyzer is promising as a body fat burn monitor for daily application at home or in gyms to provide immediate feedback during exercise and dieting for more effective body fat loss.

ASSOCIATED CONTENT

Supporting Information

The Supporting Information is available free of charge on the ACS Publications website at DOI: 10.1021/acs.analchem.7b02843.

One table and three figures containing physiological data for subjects, individual breath acetone profiles, breath acetone concentrations, and agreement analysis between sensor and PTR-TOF-MS (PDF)

AUTHOR INFORMATION

Corresponding Author

*E-mail pratsinis@ptl.mavt.ethz.ch.

ORCID

A. T. Güntner: 0000-0002-4127-752X

Notes

The authors declare no competing financial interest.

ACKNOWLEDGMENTS

This study was financially supported by the Swiss National Science Foundation (Grant 200021_159763/1). We appreciate the help of C. O. Blattmann with microscopic analysis and the Optical Materials Engineering Laboratory (Professor D. J. Norris) for providing the SEM (ETH Zürich). Support with venous blood sampling by F. Lettau and A. Stöberl and blood analysis by the Institute of Clinical Chemistry (USZ Zürich) is gratefully acknowledged. This study is part of the Hochschulmedizin Zurich flagship project Zurich Exhalomics.

REFERENCES

(1) *Global Status Report on Noncommunicable Diseases 2014*; World Health Organization, 2014; http://apps.who.int/iris/bitstream/10665/148114/1/9789241564854_eng.pdf?ua=1.

(2) The GBD Obesity Collaborators. *N. Engl. J. Med.* **2017**, *377* (1), 13−27.

(3) Murphy, K. One day, a machine will smell whether you're sick. *New York Times*, May 1, 2017; https://www.nytimes.com/2017/05/01/health/artificial-nose-scent-disease.html

(4) Kalapos, M. P. *Biochim. Biophys. Acta, Gen. Subj.* **2003**, *1621* (2), 122−139.

(5) Anderson, J. C. *Obesity* **2015**, *23* (12), 2327−2334.

(6) Gao, W.; Emaminejad, S.; Nyein, H. Y. Y.; Challa, S.; Chen, K.; Peck, A.; Fahad, H. M.; Ota, H.; Shiraki, H.; Kiriya, D.; Lien, D.-H.; Brooks, G. A.; Davis, R. W.; Javey, A. *Nature* **2016**, *529* (7587), 509−514.

(7) Risby, T. H.; Solga, S. F. *Appl. Phys. B: Lasers Opt.* **2006**, *85* (2−3), 421−426.

(8) Yamai, K.; Ohkuwa, T.; Itoh, H.; Yamazaki, Y.; Tsuda, T. *Redox Rep.* **2009**, *14* (6), 285−289.

(9) King, J.; Kupferthaler, A.; Unterkofler, K.; Koc, H.; Teschl, S.; Teschl, G.; Miekisch, W.; Schubert, J.; Hinterhuber, H.; Amann, A. *J. Breath Res.* **2009**, *3* (2), 027006.

(10) Samudrala, D.; Lammers, G.; Mandon, J.; Blanchet, L.; Schreuder, T. H.; Hopman, M. T.; Harren, F. J.; Tappy, L.; Cristescu, S. M. *Obesity* **2014**, *22* (4), 980−983.

(11) Turner, C.; Španěl, P.; Smith, D. *Physiol. Meas.* **2006**, *27* (4), 321.

(12) Spanel, P.; Dryahina, K.; Rejskova, A.; Chippendale, T. W. E.; Smith, D. *Physiol. Meas.* **2011**, *32* (8), N23−N31.

(13) Kundu, S. K.; Bruzek, J. A.; Nair, R.; Judilla, A. M. *Clin. Chem.* **1993**, *39* (1), 87−92.

(14) Toyooka, T.; Hiyama, S.; Yamada, Y. *J. Breath Res.* **2013**, *7* (3), 036005.

DOI: 10.1021/acs.analchem.7b02843
Anal. Chem. 2017, 89, 10578−10584

(15) Hagleitner, C.; Hierlemann, A.; Lange, D.; Kummer, A.; Kerness, N.; Brand, O.; Baltes, H. *Nature* **2001**, *414* (6861), 293−296.
(16) Güntner, A. T.; Koren, V.; Chikkadi, K.; Righettoni, M.; Pratsinis, S. E. *ACS Sens.* **2016**, *1* (5), 528−535.
(17) Choi, S.-J.; Lee, I.; Jang, B.-H.; Youn, D.-Y.; Ryu, W.-H.; Park, C. O.; Kim, I.-D. *Anal. Chem.* **2013**, *85* (3), 1792−1796.
(18) Hibbard, T.; Crowley, K.; Kelly, F.; Ward, F.; Holian, J.; Watson, A.; Killard, A. J. *Anal. Chem.* **2013**, *85* (24), 12158−12165.
(19) De Lacy Costello, B.; Amann, A.; Al-Kateb, H.; Flynn, C.; Filipiak, W.; Khalid, T.; Osborne, D.; Ratcliffe, N. M. *J. Breath Res.* **2014**, *8* (1), 014001.
(20) Righettoni, M.; Tricoli, A.; Pratsinis, S. E. *Chem. Mater.* **2010**, *22* (10), 3152−3157.
(21) Righettoni, M.; Tricoli, A.; Gass, S.; Schmid, A.; Amann, A.; Pratsinis, S. E. *Anal. Chim. Acta* **2012**, *738* (0), 69−75.
(22) Righettoni, M.; Tricoli, A.; Pratsinis, S. E. *Anal. Chem.* **2010**, *82* (9), 3581−3587.
(23) Mädler, L.; Roessler, A.; Pratsinis, S. E.; Sahm, T.; Gurlo, A.; Barsan, N.; Weimar, U. *Sens. Actuators, B* **2006**, *114* (1), 283−295.
(24) Herbig, J.; Titzmann, T.; Beauchamp, J.; Kohl, I.; Hansel, A. *J. Breath Res.* **2008**, *2* (3), 037008.
(25) Jordan, A.; Haidacher, S.; Hanel, G.; Hartungen, E.; Märk, L.; Seehauser, H.; Schottkowsky, R.; Sulzer, P.; Märk, T. *Int. J. Mass Spectrom.* **2009**, *286* (2), 122−128.
(26) Euler, D. E.; Dave, S. J.; Guo, H. *Clin. Chem.* **1996**, *42* (2), 303−308. http://clinchem.aaccjnls.org/content/clinchem/42/2/303.full.pdf.
(27) Pellegrino, R.; Viegi, G.; Brusasco, V.; Crapo, R. O.; Burgos, F.; Casaburi, R.; Coates, A.; van der Grinten, C. P. M.; Gustafsson, P.; Hankinson, J.; et al. *Eur. Respir. J.* **2005**, *26* (5), 948−968.
(28) Tassopoulos, C.; Barnett, D.; Fraser, T. R. *Lancet* **1969**, *293* (7609), 1282−1286.
(29) Swain, D. P.; Abernathy, K. S.; Smith, C. S.; Lee, S. J.; Bunn, S. A. *Med. Sci. Sports Exercise* **1994**, *26* (1), 112−116.
(30) Güntner, A. T.; Pineau, N. J.; Chie, D.; Krumeich, F.; Pratsinis, S. E. *J. Mater. Chem. B* **2016**, *4* (32), 5358−5366.
(31) Güntner, A. T.; Righettoni, M.; Pratsinis, S. E. *Sens. Actuators, B* **2016**, *223*, 266−273.
(32) Barsan, N.; Weimar, U. *J. Electroceram.* **2001**, *7* (3), 143−167.
(33) Staerz, A.; Berthold, C.; Russ, T.; Wicker, S.; Weimar, U.; Barsan, N. *Sens. Actuators, B* **2016**, *237*, 54−58.
(34) Wang, L.; Teleki, A.; Pratsinis, S. E.; Gouma, P. I. *Chem. Mater.* **2008**, *20* (15), 4794−4796.
(35) Righettoni, M.; Schmid, A.; Amann, A.; Pratsinis, S. E. *J. Breath Res.* **2013**, *7* (3), 037110.
(36) Righettoni, M.; Ragnoni, A.; Güntner, A. T.; Loccioni, C.; Pratsinis, S. E.; Risby, T. H. *J. Breath Res.* **2015**, *9* (4), 047101.
(37) Anderson, J. C.; Lamm, W. J. E.; Hlastala, M. P. *J. Appl. Physiol.* **2006**, *100* (3), 880−889.
(38) Di Francesco, F.; Loccioni, C.; Fioravanti, M.; Russo, A.; Pioggia, G.; Ferro, M.; Roehrer, I.; Tabucchi, S.; Onor, M. *J. Breath Res.* **2008**, *2* (3), No. 037009.
(39) Jones, A. *J. Anal. Toxicol.* **1987**, *11* (2), 67−69.
(40) Bland, J. M.; Altman, D. G. *Lancet* **1986**, *327* (8476), 307−310.

DOI: 10.1021/acs.analchem.7b02843
Anal. Chem. 2017, 89, 10578−10584